Journal of Ceramic Processing Research. Vol. 17, No. 12, pp. 1254~1259 (2016)

J O U R N A L O F
Ceramic Processing Research

Synthesis and properties of sol-gel derived transparent ZnO thin films: Effect of indium doping

Eyüp Fahri Keskenler[a,*] and Güven Turgut[b]

[a]*Department of Material Science and Nanotechonology, Recep Tayyip Erdoğan University, Faculty of Engineering, 53100 Rize, Turkey*
[b]*Faculty of Basic Sciences, Department of Physics, Erzurum Technical University, 25240 Erzurum, Turkey*

High quality and transparent indium doped ZnO (IZO) thin films were deposited on glass substrates by sol-gel spin coating method. Zinc acetate and indium (III) chloride were used as precursor solution materials. Structural, morphological, and optical properties of the films were investigated as a function of indium doping ranging from 0.5% to 2.0 at % by X-ray diffraction, scanning electron microscopy, transmission and energy dispersive X-ray techniques. The films had polycrystalline nature and exhibited a hexagonal wurtzite structure with preferred c-axis orientation. The film surfaces exhibited uniform particle-like and granular morphologies. The optical transmittance spectra of the undoped ZnO and IZO films were taken in the wavelength ranging from 350-1000 nm. The transmittance IZO films compared to undoped ZnO has increased with increasing indium content. The chemical composition of the films indicated the presence of indium element in the ZnO films. These results make IZO thin films an attractive candidate for transparent material applications such as solar cells.

Key words: In doped ZnO, ZnO, Sol-gel, Optical and structural properties, TCOs.

Introduction

Transparent conducting oxides (TCOs), such as zinc oxide (ZnO), indium tin oxide (ITO), indium oxide (In_2O_3) and tin oxide (SnO_2) have recently been studied for applications related to microelectronics and optoelectronics fields including thin film sensor, transistors and solar cells [1-3]. Among these TCO candidates, ZnO is a promising material with properties of low resistivity, a large exciton binding energy (60 meV), a strong cohesive energy (1.89 eV) and a direct wide bandgap (3.37 eV) at room temperature [4, 5]. It has also high optical gain and transmittance in the visible range [6], high mechanical and thermal stabilities [7] and high light trapping characteristics [8]. Because of these properties, ZnO being from II-VI semiconductor group has been extensively studied for its advantages of application in light emitting diodes (LEDs) [9], laser diodes [10], transparent electrodes [11], surface acoustic devices [12] and flat panel displays [13]. ZnO films have *c*-axis orientations with hexagonal wurtzite crystal structure and can be smoothly deposited on various kinds of substrates such as glass, Si, sapphire, etc. Besides all these, it is economical and environmental material due to non-toxity, inexpensive cost and to be found easily in nature [14]. Different dopant ions with the desirable concentration can be used to obtain conducting and transparent ZnO thin films. The metal dopants (Sn^{4+}, In^{3+}, Al^{3+}, Zr^{2+}, Mn^{2+}, Ga^{+}, etc.) improving the electrical and optical properties of ZnO were reported in several studies [15-17]. In general, the ZnO doping is intended to displacement of Zn atoms (Zn^{+2}) with atoms of higher valance elements such as Aluminum (Al^{+3}), Indium (In^{+3}), Tin (Sn^{+4}) and, obtain the native defect or impurity atoms which are changing the electrical conduction and optical properties [8, 18].

Doped and undoped ZnO thin films have been synthesized using several techniques such as sputtering [19], vacuum evaporation [20], pulsed laser deposition (PLD) [21], molecular beam epitaxy (MBE) [22, 23], chemical spray pyrolysis (CSP) [24], Successive Ionic Layer Adsorption Reaction (SILAR) [25], metal-organic chemical vapor deposition (MOCVD) [26] sol-gel method [27-29] and etc. Among these, sol-gel is one of the most useful methods and compared with the others, it has some advantages such as simple and practical process, low cost and temperature, controllable solution concentrations and dopants, obtaining intended film thickness, and smooth-surface films [30].

Although there are several reports on doping of ZnO with aluminum [31], lithium [32], gallium [33], nickel [34] and tin [35], many research groups [36-41] have recently investigated the structural, optical and electrical properties of IZO thin films because of its good conductivity and higher optical transmittance. Benouis et al. [42] have investigated the effect of indium doping on structural, electrical conductivity, photoconductivity and density of states properties of ZnO thin films grown by spray pyrolysis method and found that In doping had an important effect on the electronic and optical properties. The IZO thin film having 2% doping level had exhibited

*Corresponding author:
Tel : +90-464-2236126 / 1235, 90-537-6104849
E-mail: keskenler@gmail.com

the lowest resistivity compared to undoped ZnO.

Until now, there are little reports on the studies involving In doped ZnO (IZO) thin film synthesized by sol-gel spin coating method [43-46]. Chen et al. [43] have examined the temperature effects and the contribution of indium dopants on crystallization mechanism of ZnO nanostructures. Both improvements of the ZnO crystallization quality and significantly growth of ZnO nano-pillars have been observed with increasing the crystallizing temperature. As a function of the film thickness and the post-deposition annealing treatments in different atmospheres, the electrical resistivity, structure, morphology and optical transmittance of the films were investigated by the Arredondo et al. [44] and Girtan et al. [47]. Abdullah et al. [45] have observed that the crystal quality of the IZO films was highly dependent on the annealing temperature and could be improved along with the films annealed from 400 ºC to 600 ºC.

In the present paper, we describe the effects of In doping on structural, morphological and optical properties of sol-gel synthesized ZnO thin films. Since the technique used here for the film preparation is very simple, it is quite easy to vary the doping concentrations in this technique and hence one can vary the properties of the films.

Experimental Details

The thin film deposition was performed by sol-gel spin-coating method on glass substrate, using a sol prepared with zinc acetate dihydrate ($Zn(CH_3COO)_2 \cdot 2H_2O$), indium(III) chloride ($InCl_3$), monoethanolamine (C_2H_7NO, MEA) and 2-methoxyethanol ($C_3H_8O_2$), as starting material, dopant source, stabilizer and solvent, respectively. The molar ratio of MEA to metal salts was maintained at 1 : 1. 0.5 M zinc acetate dihydrate and 0.5 M indium(III) chloride were mixed in different solution mole ratios from 0.5 at % mole to 2.0 at % mole. The IZO films were identified according to indium content as 0.5% IZO, 1.0% IZO and 2.0% IZO and undoped ZnO (a reference sample). The precursor sol was stirred at 100 ºC for 24 hrs in a tightly-closed flask to obtain a clear and homogenous solution. The glass substrates were cleaned in acetone and methanol by using an ultrasonic cleaner and dipped in diluted 10% HF (hydrofluoric acids) for 30 sec. Then the substrates were rinsed with de-ionized (DI) water and dried with nitrogen. The resultant solution was dropped on glass substrate and then spin coated at a speed of 3000 rpm for 25 sec. After spin coating, the films were dried at 250 ºC for 5 min to remove the solvent and organic residuals and then allowed to cool down to room temperature. This procedure was repeated for 10 times to obtain the intended thickness and film quality. The same procedure was repeated for the films prepared with different values of fluorine doped and finally, they were annealed in air at 500 ºC for 30 min. X-ray diffraction (XRD) patterns were taken using a Rigaku D/Max-IIIC diffractometer. The diffractometer reflections were investigated at room temperature and the values of 2θ were altered between 20 º and 85 º. The incident wavelength was 1.5418 Å. Morphological properties of the films were determined with Nova Nanosem 430. The optical absorbance of the thin films was recorded in spectral region of 350-1000 nm at 300 K using a UV-VIS spectrophotometer (Perkin-Elmer, Lambda 35) which works in the range of 200-1100 nm and has a wavelength accuracy of better than ± 0.3 nm.

Results and Discussion

The crystal structure and orientation of undoped ZnO and IZO thin films having different In concentrations were investigated by XRD patterns. Fig. 1 shows the XRD patterns of undoped and IZO films deposited at different In dopant concentrations on the glass substrate. The ZnO films normally crystallized with the hexagonal wurtzite structure and a preferred orientation of (002). But, these spectra indicate that the films have polycrystalline nature and the peak positions fit well with a hexagonal wurtzite ZnO structure (JCPDS card file no. 36-1451) and no phases related to In have been observed in the IZO films. As can be seen in Fig. 1, doping of ZnO with the different In concentrations did not affect the crystallization of ZnO films except getting reduced the diffraction peaks indicating the IZO films lower crystallinity as compared with the undoped ZnO films. Even if the preferential orientation peak is (002), weak

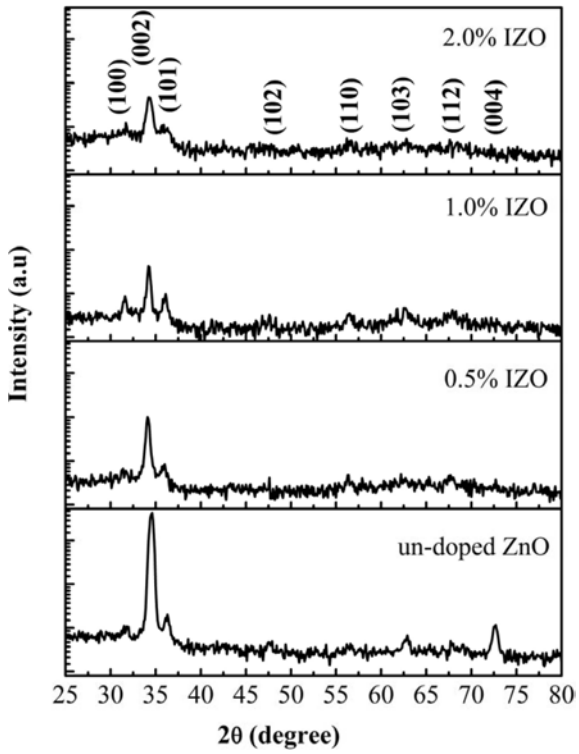

Fig. 1. XRD patterns of ZnO thin films with different indium contents.

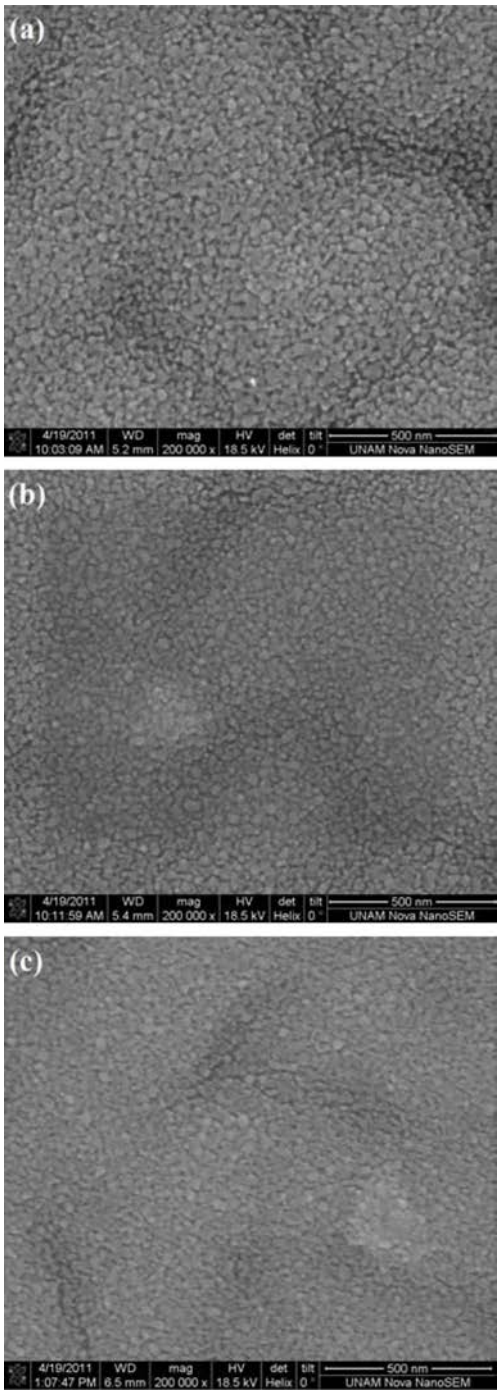

Fig. 2. SEM micrographs of indium-doped zinc oxide films (a) 0.5% IZO, (b) 1.0% IZO and (c) 2.0% IZO.

intensity peaks corresponding to (100), (101), (110), (103), (102), (112) and (004) along with (002) were also observed for undoped ZnO film. Although the maximum preferential peak intensities were observed for undoped ZnO film, with the In concentration increasing, the intensity of all diffraction peaks decreased even for the dominant (002) peak, and (102), (112) and (004) peaks were completely vanished at 2% mole In concentration. Similar results were also observed by Girtan et al. and Kumar et al. [38, 47].

The surface morphology of the films was investigated with SEM. The thickness of the films was estimated from cross-sectional SEM images and it was found to be 0.42mm. From the results of SEM analysis shown in Fig. 2 (a-c), it is quite clear that the surface nature of the films is greatly affected by the indium dopant concentration. The film surfaces exhibited uniform particle-like and granular morphologies. It has been pointed out by many groups that sol-gel derived thin films exhibited most likely particle-like surface [48-50]. This particle-like structures were similar to ones that seen by Chen et al. [15] and Chakraborty et al. [51]. When indium (III) chloride was used as dopant, the grains were observed to be well defined and uniformly distributed over the surface. In addition, it is clearly obvious that increasing doping concentration from 0.5% to 2.0% have reduced the grain sizes in IZO films.

The calculated interplanar distance '*d*' values from XRD analysis have been given in Table 1. The difference in interplanar distance between standard values obtained from JPDS card no: 36-1451 and calculated values for undoped and IZO films deposited at different In dopant concentrations is very small. The almost matched values of the calculated and standard '*d*' confirms that the deposited films are ZnO with a hexagonal wurtzite structure. Nearly the same results for the (100), (002) and (101) peaks were also reported by Nirmala and Anukaliani [52] for 5 and 10 at % Co doped ZnO films.

The calculated lattice parameters and crystallite sizes have been given in Table 2 along with the standard values obtained from JPCDS card no: 36-1451. The lattice constants '*a*' and '*c*' of the wurtzite structure of ZnO were calculated using the following relations [53];

$$\frac{1}{d^2}=\frac{4}{3a^2}(h^2+hk+k^2)+\frac{l^2}{c^2} \quad (1)$$

Where '*d*' is the interplanar distance and (*hkl*) is miller indices, respectively. It is seen from Table 2 that as the doping concentration increases the values of lattice parameters 'a' and'c' increase for 0.5% IZO compared

Table 1. Standard and calculated interplanar distances 'd' values of the films.

(hkl)	Standard d (Å)	Calculated d (Å)			
		0.0 % IZO	0.5 % IZO	1.0 % IZO	2.0 % IZO
100	2.814	2.837	2.829	2.832	2.819
002	2.603	2.592	2.618	2.626	2.617
101	2.475	2.473	2.486	2.484	2.479
102	1.911	1.911	1.913	1.916	–
110	1.624	1.623	1.628	1.631	1.626
103	1.477	1.476	1.481	1.483	1.479
112	1.378	1.384	1.381	1.386	–
004	1.301	1.299	1.299	1.302	–

Table 2. The structural parameters of undoped and In doped ZnO thin films.

Sample (% mole In doped)	Lattice constants (Å)		D (nm)	N ($\times 10^{16}$m^{-2})	(100)/(002)	(101)/(002)
	a	c				
0.0	3.249	5.183	16.17	9.88	0.07561	0.09823
0.5	3.262	5.236	20.54	4.81	0.30615	0.33966
1.0	3.273	5.252	18.44	6.65	0.49837	0.52683
2.0	3.255	5.236	14.56	13.52	0.55271	0.53333

JPDS card no: 36-1451 (a = 3,250 Å c* = 5,207 Å).

to undoped ZnO (a = 3.249 nm; c = 5.183 nm) to 3.262nm and and 5.236 nm, respectively, then again increases onwardly to 3.273 nm and 5.252nm for 1.0% IZO. Interestingly for 2.0% IZO they decrease to 3.255 nm and 5.236nm. The crystallite sizes of the undoped ZnO and IZO films deposited at different In dopant concentrations were calculated by using Scherrer's formula [54];

$$D = \frac{0.9\ \lambda}{\beta \cos(\theta)} \quad (2)$$

Where λ is the wavelength of the X-ray, β is the full width at half maximum (FWHM) of the diffraction peak in radians and θ is Bragg diffraction angle. The average crystallite size of the undoped ZnO is found to be 16.17 nm, and for 0.5, 1.0 and 2.0 at % In doped ZnO, the average size is found to be 20.54 nm, 18.44 nm and 14.56 nm, respectively. It is seen that, compared with undoped ZnO, 0.5 at % In doped ZnO films resulted in an maximum increase in crystallite size revealing that it has highest crystallite size. The chance in crystallite size is in very good agreement with SEM micrographs in Fig. 2. The number of crystallites per unit area (N) of the films was determined using the following relation [55] and given in Table 2;

$$N = \frac{t}{D^2} \quad (3)$$

Where *t* is the thickness of the film. As can be seen in Table 2, there is a conversely relation between the crystallite size and the number of crystallite per unit area. Although 0.5% IZO film has the maximum average crystallite size of 20.54 nm among the IZO films, it has the minimum number of crystallites per unit area of 4.81×10^{16}m^{-2}. Ratio of peak intensities for (100) / (002) and (101) / (002) planes of undoped and IZO films were also calculated and given in Table 2. As can be seen in Table 2 that in undoped ZnO film (100) / (002) and (101) / (002) ratios have the lowest values indicating highest orientation of c-axis in undoped ZnO. However IZO films show increase in these ratios with increase in indium concentration [56].

The optical transmittance spectra of the undoped ZnO and IZO films in the wavelength ranging from 350-1000 nm is shown in Fig. 3. As can be seen in the transmittance spectra of undoped ZnO and IZO films, the transmittance is increased with increasing In content and All the films are

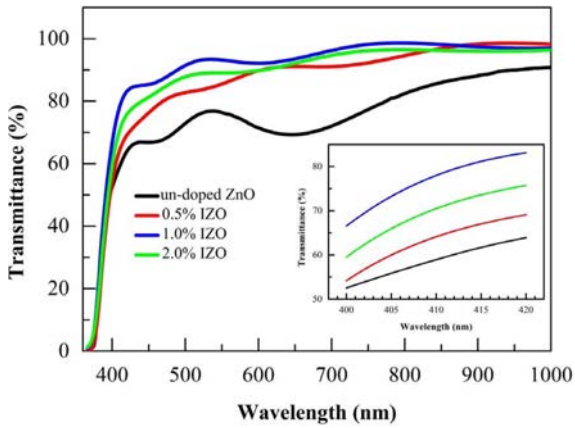

Fig. 3. Optical transmittance spectra of the undoped ZnO and IZO films in the wavelength range of 350-1000 nm.

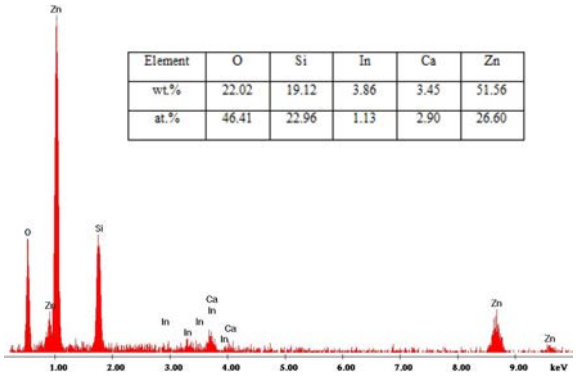

Fig. 4. A typical EDX spectrum of 2.0 at % In doped ZnO thin film.

highly transparent in the visible region. The transmission spectra show interference fringes for all the films. The appearance of interference fringes indicates the smooth reflecting surface of the films and minimum scattering loss at the surface, which indirectly proved the homogeneous film deposition. A typical transmittances of 93.17, 89.07, 85.46 and 76.37% at 550nm were obtained for 1.0, 2.0, 0.5 at % In doped ZnO films and undoped ZnO, respectively. It is quite clear from the transmittance spectra that the IZO films had better transparency than undoped ZnO film and this behavior has also been observed by Kumar et al. [38]. The transmittance shows firstly increasing tendency with increasing In concentration and reached a maximum value of the 1.0 at % In doped ZnO,

then shows a decreasing with 2.0 at % In doped ZnO. The transmittance in the visible region decreased at short wavelengths near the ultraviolet range. The inset figure shows the transmittances values in the range of 400-420 nm wavelength. The chemical composition of the films was determined by energy-dispersive X-ray (EDX) spectroscopy and given in Fig. 4 for 2.0 at % In doped ZnO. Fig. 4 indicates the presence of O, Si, In, Ca and Zn elements and shows that In content in the film is 3.52 at.% which gives the direct evidence that In atoms are introduced into the ZnO. The Si and Ca peaks are related to the glass substrate.

Conclusions

In this study, high quality transparent indium doped ZnO (IZO) thin films were deposited on glass substrate by sol-gel spin coating method and their structural, morphological, and optical properties were investigated as a function of indium doping. Although the preferential orientation peak was (002), other peaks like (100), (101), (110), (103), (102), (112) and (004) were also observed. The intensity of all diffraction peaks decreased with increasing the In content. SEM images showed that the film surfaces exhibited uniform particle-like and granular morphologies and were affected by the indium incorporation. Increasing doping concentration from 0.5% to 2.0% have reduced the grain sizes in IZO films. There were almost no difference in interplanar distance between standard and calculated values for the films. This is indication of the growth of the ZnO films having a hexagonal wurtzite structure. All the films were highly transparent in the visible region. The fact that the transmittance increased with increasing In content and the IZO films had better transparency than undoped ZnO film makes IZO films as a candidate for transparent material applications such as solar cells.

References

1. S. Faÿ, J. Steinhauser, S. Nicolay, C. Ballif, Thin Solid Films 518 (2010) 2961.
2. J.-W. Hoon, K.-Y. Chan, J. Krishnasamy, T.-Y. Tou, D. Knipp, Appl. Surf. Sci. 257 (2010) 2508-2515.
3. R. Khandelwal, A.P. Singh, A. Kapoor, S. Grigorescu, P. Miglietta, N.E. Stankova, A. Perrone, Opt. and Laser Technol. 40 (2008) 247.
4. Ü. Özgür, Ya.I. Alivov, C. Liu, A. Teke, M.A. Reshchikov, S. Dogan, V. Avrutin, S.-J. Cho, H. Morkoç, J. Appl. Phys. 98 (2005) 041301.
5. O. Lupan, T. Pauporté, L. Chow, B. Viana, F. Pellé, L.K. Ono, B. Roldan Cuenya, H. Heinrich, Appl. Surf. Sci. 256 (2010) 1895.
6. T.V. Vimalkumar, N. Poornima, C.S. Kartha, K.P. Vijayakumar, Mater. Sci. and Eng. B-Adv. 175 (2010) 29.
7. J.J. Ding, H.X. Chen, S.Y. Ma, Appl. Surf. Sci. 256 (2010) 4304.
8. Y. Caglar, S. Ilican, M. Caglar, F. Yakuphanoglu, Spectrochim. Acta A 67 (2007) 1113.
9. M. Jiang, X. Liu, H. Wang, Surf. Coat. Tech. 203 (2009) 3750.
10. Y.J. Zhang, J.B. Wang, X.L. Zhong, Y.C. Zhou, X.L. Yuan, T. Sekiguchi, Solid State Commun. 148 (2008) 448.
11. Y.-S. Kim, W.-P. Tai, Appl. Surf. Sci. 253 (2007) 4911.
12. D.C. Agarwal, D.K. Avasthi, F. Singh, D. Kabiraj, P.K. Kulariya, I. Sulania, J.C. Pivin, R.S. Chauhan, Surf. Coat. Tech. 203 (2009) 2427.
13. S. Goldsmith, Surf. Coat. Tech. 201 (2006) 3993.
14. N. Bahadur, A.K. Srivastava, S. Kumar, M. Deepa, B. Nag, Thin Solid Films 518 (2010) 5257.
15. K.J. Chen, F.Y. Hung, S.J. Chang, Z.S. Hu, Appl. Surf. Sci. 255 (2009) 6308.
16. Y.C. Lin, B.L. Wang, W.T. Yen, C.T. Ha, Chris Peng, Thin Solid Films 518 (2010) 4928.
17. R.K. Gupta, K. Ghosh, P.K. Kahol, Appl. Surf. Sci. 256 (2009) 1538.
18. P. Sagar, M. Kumar, R.M. Mehra, Solid State Commun. 147 (2008) 465.
19. S.H. Seo, H.C. Kang, Thin Solid Films 518 (2010) 6446.
20. S. Naseem, M. Iqbal, K. Hussain, Sol. Energy Mater. Sol. Cells 31 (1993) 155.
21. L.H. Van, M.H. Hong, J. Ding, J. Alloy. Compd. 449 (2008) 207.
22. Y.F. Chen, N.T. Tuan, Y. Segawa, H.J. Ko, S.K. Hong, T. Yao, Appl. Phys. Lett. 78 (2001) 1469.
23. Z.K. Tang, G.K.L. Wong, P. Yu, M. Kawasaki, A. Ohtomo, et al., Appl. Phys. Lett. 72 (1998) 3270.
24. P.P. Sahay, R.K. Nath, Sensor Actuat. B – Chem. 134 (2008) 654.
25. P.S. Kumar, A.D. Raj, D. Mangalaraj, D. Nataraj, Thin Solid Films 518 (2010) e183.
26. E. Chikoidze, M. Nolan, M. Modreanu, V. Sallet, P. Galtier, Thin Solid Films 516 (2008) 8146.
27. L. Xu, X. Li, J. Yuan, Superlattice Microst. 44 (2008) 276.
28. D. Wang, J. Zhou, G. Liu, J. Alloy. Compd. 481 (2009) 802.
29. Y. Caglar, S. Ilican, M. Caglar, F.Yakuphanoglu, J. Sol-Gel Sci. Techn. 53 (2010) 372-377.
30. H. Abdullah, M.N. Norazia, S. Shaari, J.S. Mandeep, Thin Solid Films 518 (2010) e174.
31. N.F.Y. Cooray, K. Kushiya, A. Fujimaki, D. Okumura, M. Sato, M. Ooshita and O. Yamase, Japan J. Appl. Phys. 38 (1999) 6213.
32. A. Ortiz, C. Falcony, A.J. Hernandez, M. Garcia and J.C. Alonso, Thin Solid Films 29 (1997) 103.
33. M. de la L. Olvera and A. Maldonado, Phys. Status Solidi A 196 (2003) 410.
34. K.-T. Kim, G.-H. Kim, J.-C. Woo, C.-I. Kim, Surf. Coat. Tech. 202 (2008) 5650-5653.
35. S.Y. Bae, C.W. Na, J.H. Kang, J. Park, J. Phys. Chem. B 109 (2005) 2526-2531.
36. S. M. Rozati, F. Zarenejad, and N. Memarian, Thin Solid Films doi:10.1016/j.tsf.2011.04.200 (2011)
37. E. P´al, I. D´ek´any, Colloid Surface A: Physicochem. Eng. Aspects 318 (2008) 141-150.
38. P.M.R. Kumar, C.S. Kartha, K.P. Vijayakumar, T. Abe, Y. Kashiwaba, F. Singh and D.K. Avasthi, Semicond. Sci. Technol. 20 (2005) 120-126.
39. J.H. Lee, S.Y. Lee, B.O. Park, Mater. Sci. Eng. B 127 (2006) 267-271.
40. M. Miki-Yoshida, F. Paraguay-Delgado, W. Estrada-Lopez and E. Andrade, Thin Solid Films 376 (2000) 99.
41. E.P. Zironi, J. Ca˜netas-Ortega, H. Gomez, A. Maldonado, R. Asomoza and J. Palacios-Gomez, Thin Solid Films 293

(1997) 117.
42. C.E. Benouis, M. Benhaliliba, A. Sanchez Juarez, M.S. Aida, F. Chami and F. Yakuphanoglu, J. Alloy. Compd. 490 (2010) 62-67.
43. K.J. Chen, F.Y. Hung, S.J. Chang, S.J. Young, Z.S. Hu, Curr. Appl. Phys. 11 (2011) 1243-1248.
44. E.J. Luna-Arredondo, A. Maldonado, R. Asomoza, D.R. Acosta, M.A. Mele´ndez-Lira, M. de la L. Olvera, Thin Solid Films 490 (2005) 132-136.
45. H. Abdullah, M.N. Norazia, S. Shaari, J.S. Mandeep, Thin Solid Films 518 (2010) e174-e180.
46. K.J. Chen, F.Y. Hung, S.J. Chang, Z.S. Hu, Appl. Surf. Sci. 255 (2009) 6308-6312.
47. M. Girtan , M. Socol, B. Pattier, M. Sylla, A. Stanculescu, Thin Solid Films 519 (2010) 573.
48. J.H. Lee, K.H. Ko, B.O. Park, J. Cryst. Growth 247 (2003) 119.
49. H.M. Zhou, D.Q. Yi, Z.M. Yu, L.R. Xiao, J. Li, Thin Solid Films 55 (2007) 6909.
50. K.J. Chen, T.H. Fang, F.Y. Hung, L.W. Ji, S.J. Chang, S.J. Young, Y.J. Hsiao, Appl. Surf. Sci. 254 (2008) 5791.
51. A. Chakraborty, T. Mondal, S.K. Bera, S.K. Sen, R. Ghosh, G.K. Paul, Mater. Chem. Phys. 112 (2008) 162.
52. M. Nirmala, A. Anukaliani, Physica B 406 (2011) 911-915.
53. A. Sakthivelu, V. Saravanan, M. Anusuya, J.J. Prince, J. of Ovonic Research 7 (2011) 1.
54. A. Bowen, J. Li, J. Lewis, K. Sivaramakrishnan, T.L. Alford, S. Iyer, Thin Solid Films 519 (2011) 1809.
55. K. Ravichandran, B. Sakthivel, and P. Philominathan, Cryst. Res. Technol. 45 (2010) 292-298.
56. S.S. Badadhe, I.S. Mulla, Sensor. Actuat. B-Chem. 143 (2009) 164-170.